Backwards Maneuvering Powered Wheelchairs with Haptic Guidance

Emmanuel B. Vander Poorten, Eric Demeester, Alexander Hüntemann, Eli Reekmans, Johan Philips, and Joris De Schutter

KU Leuven, Dept. of Mechanical Engineering,
Celestijnenlaan 300B, 3001 Heverlee, Belgium
{emmanuel.vanderpoorten,eric.demeester,alexander.huntemann, johan.philips,joris.deschutter}@mech.kulueven.be,
{eli.reekmans}@intermodalics.eu
http://www.mech.kuleuven.be

Abstract. This paper describes a novel haptic guidance scheme that helps powered wheelchair users steer their wheelchair through narrow and complex environments. The proposed scheme encodes the local environment of the wheelchair as a set of collision-free circular paths. An adaptive impedance controller is constructed upon these circular paths. The controller increases resistance when nearing obstacles and simultaneously helps the user to change motion towards a safer circular path. To test the algorithm, a commercial powered wheelchair was interfaced and equipped with necessary sensors and an in-house built haptic joystick. The user was asked to drive backwards into a narrow elevator with and without navigation assistance. Although there is still room for improvements, the first results are promising. Thanks to the assistance the user can perform this maneuver successfully in most of the cases without even looking backwards.

Keywords: haptic guidance, navigation assistance, robotic wheelchair, shared control.

1 Introduction

Accurately steering vehicles backwards, e.g. for parking or maneuvering, remains a non-trivial, error-prone task. Since 2003 where Toyota sold the first intelligent park assist system in the Toyota Prius, more and more car manufacturers promote similar park assist systems. These devices help drivers when executing parallel parking maneuvers. Typically the user keeps the control over the velocity, while steering is managed by the car. While the need for assistance during backwards maneuvers with powered wheelchairs is presumably much higher than for cars, as many users have big trouble even looking backwards in their chair, manufacturers of powered wheelchairs are not that far as their counterparts in the automotive sector. The large difference in market size and available budget explains to a large extent the development delay. Further explanations can be found in the different vehicle kinematics, the large variability in environmental conditions compared to the more or less structured car parking tasks, but also the large variability in level of expertise and capability of the drivers. Powered wheelchair drivers form a very heterogeneous public covering people with physical

P. Isokoski and J. Springare (Eds.): EuroHaptics 2012, Part I, LNCS 7282, pp. 419–431, 2012.

and/or cognitive disabilities with varying level of expertise. Navigation assistance systems that help during navigation should account for this large variability and be able to cope with it in a reliable manner. The above elements explain why car technology cannot be simply transferred to wheelchair navigation assistance.

One seemingly appealing manner to overcome the large heterogeneity in the population of wheelchair users would lie in the development of technology to execute maneuvering tasks fully autonomously, thus without the need for user interventions. While this might from a technological point of view become possible, from the point of view of the user this is not always attractive. People in general, and people with disabilities in particular, like to be in control. The knowledge to be capable of executing quite complex tasks can boost moral. This is the case for youngsters who are eager to learn and gain control or for older people that might be afraid to loose control. For people with multiple sclerosis or dementia for example exposure to challenging navigation tasks may help them remain capable and alert, whereas the absence of stimuli might speed up degradation of earlier competences. Also providing too good assistance might have a detrimental effect [1]. The final goal of the EC-funded FP7 project RADHAR (`http://www.radhar.eu`), which stands for Robotic ADaptation to Humans Adapting to Robots, exists in developing technology that allows automatic adjustment of the level of navigation assistance adapted to each specific user at each instant in time. This assistive technology should enable the user to execute complex navigation tasks in a safe, intuitive and rewarding manner.

This paper describes a novel haptic guidance scheme that was developed within the framework of RADHAR project that helps users maneuver backwards with a powered wheelchair. The assistance simplifies the navigation, while keeping the user in full control of the wheelchair. The layout of the paper is organised as follows: section 2 summarizes briefly the major principles of steering commercial powered wheelchairs; section 3 reviews a number of efforts described in literature that provide navigation assistance to powered wheelchair drivers. The difference between what we like to call ‘unilateral’ and ‘bilateral’ assistance schemes is shortly explained. Section 4 describes a novel bilateral navigation assistance scheme that haptically guides the user along collision-free paths. Experimental results of this control scheme are presented and discussed in section 5. Finally, conclusions are drawn and directions for future work are sketched in 6.

2 Powered Wheelchair Navigation Principles

Powered wheelchairs are non-holonomic vehicles that are operated by various types of input devices ranging from proportional manual joysticks, over chin or tongue joysticks towards scanning eye-tracking devices [2] or even exotic brain computer interfaces [3]. This section gives a rough sketch of the basic operating principle of powered wheelchairs through proportional manual joysticks. These two-dimensional joysticks are most commonly used in practice as input devices. The navigation assistance schemes developed further on in this paper rely on a haptic variant of a traditional 2DOF joystick.

2.1 Non-holonomicity of Powered Wheelchair

Similar to cars, commercial powered wheelchairs are non-holonomic vehicles, some exceptions (e.g. [4]) left out of consideration. Dissimilar to cars is the type of non-holonomicity. Powered wheelchairs have two driven wheels, the velocity (ω_1, ω_2) of which is controlled separately. When both wheels rotate at the same speed, assuming equal wheel diameters, the wheelchair moves on a straight line. When both wheels rotate at the same speed but in opposite direction, the wheelchair turns on the spot. This relation is expressed as

$$v_{wch} = r_{wheel}(\omega_1 + \omega_2)/2, \tag{1}$$

$$\omega_{wch} = r_{wheel}(\omega_1 - \omega_2)/B_{ax}. \tag{2}$$

Here v_{wch} and ω_{wch} are respectively the translational and rotational velocity of the wheelchair expressed in a local wheelchair coordinate frame Σ_{wch}. The frame Σ_{wch} is rigidly attached to the wheelchair in the center between the two driven wheels (see Fig.1). The distance between both driven wheels along the wheel axis is B_{ax}. r_{wheel}, the wheel radius, for the left and right wheel is assumed equal and constant for simplicity. Depending on the type of wheelchair front-, mid- or back-wheels are actuated. The non-actuated wheels, often refered to as castor wheels, stabilise the wheelchair but also disturb the idealized relations (1) and (2). Wheel slippage, pressure variations in tires and other dynamic effects are other factors that affect the navigation. For reasons of simplicity all these disturbance factors are not accounted for in this work and relations (1) and (2) are employed.

2.2 Mapping of Joystick Deflection to Wheelchair Motion

The most straightforward manner to operate a non-holonomic wheelchair is probably by employing a traditional proportional manual joystick, with a linear relation between joystick deflection and commanded wheelchair speed. This mapping is conceptually depicted in Fig.1. For a joystick deflection (x_j, y_j) expressed in coordinate system frame Σ_j attached to the joystick base, the commanded wheelchair rotational and translational velocity are:

$$v_{wch} = k_v y_j, \tag{3}$$

$$\omega_{wch} = -k_\omega x_j \tag{4}$$

with appropriate velocity gains k_v and k_ω. When maintaining this particular joystick position over a longer period of time, the wheelchair will follow a circular trajectory $\mathscr{C}_m$, expressed in a base reference frame Σ_b with radius given by:

$$r_{wch} = |v_{wch}|/|\omega_{wch}|. \tag{5}$$

When ignoring the dynamic effects of the wheelchair, a general wheelchair trajectory can be approximated as a sequence of instantaneous motions on circular paths $\mathscr{C}_m$ that follow joystick motions (x_j, y_j) over time. The traversal speed along the circular path is proportional to the joystick deflection amplitude $r_j = \sqrt{x_j^2 + y_j^2}$. It is straightforward

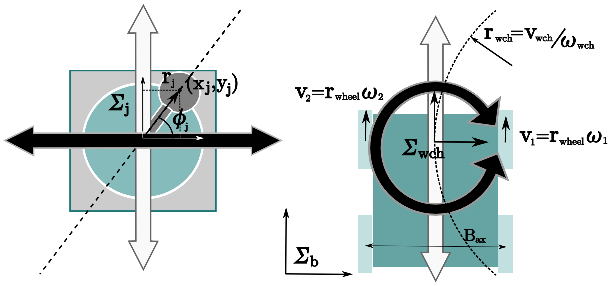

Fig. 1. One to one mapping of joystick position (left) to wheelchair velocity (right). Each position (x_j, y_j) expressed in frame Σ_j corresponds to a linear and rotational velocity (v_{wch}, ω_{wch}) w.r.t. the local wheelchair coordinate frame Σ_{wch}, resulting in an instantaneous circular path with radius $r_{wch} = v_{wch}/\omega_{wch}$ in base coordinate frame Σ_b.

to verify that for all joystick positions forming a constant angle $\phi_j + i\pi$, $i = \{0,1\}$ with the horizontal X-axis of Σ_j, the wheelchair will move along the same circular path $\mathscr{C}_m$, albeit with different speeds. By extension, all two-dimensional joystick positions can be encoded in such way to a one-dimensional set of circular paths. For computational reasons a discrete number of paths with radius r^m_{wch} is employed:

$$r^m_{wch} = \left| \frac{k_v}{k_\omega} \tan(m\Delta\phi) \right|, \quad \text{for } m = 0, \ldots, N-1 \text{ and } N \in \mathbb{Z}^+_0$$
$$\text{and} \quad \Delta\phi = \frac{2\pi}{N-1} \quad \text{where } N \to \infty. \tag{6}$$

Each circular path segment is represented as a (v, ω, dt) tuple where the path's length equals $v \cdot dt$ and the orientation change $\omega \cdot dt$. $m\Delta\phi = \{0, \pi\}$ corresponds to pure rotational motion, whereas $m\Delta\phi = \{\pi/2, 3\pi/2\}$ corresponds to pure translational motion.

Note that mapping (3-4) requires a user who wants to drive backwards to the right to hold his/her joystick to the left. This is quite counterintuitive and complicates delicate back and forth maneuvering. Some wheelchair manufactures therefore foresee an opposite mapping for backwards motion.

3 Navigation Assistance for Powered Wheelchairs

Maneuvering powered wheelchairs and more in particular maneuvering such devices backwards remains a challenging and potentially dangerous task, even for experienced wheelchair users. Seemingly simple and frequently occuring maneuvers like door-passing or taking an elevator require in reality considerable motor and cognitive skills. The relatively large dimensions of wheelchairs compared to the size of the environment, the limited response speed and large inertia can lead to dangerous situations, possibly inflicting serious harm upon driver, bystanders or damage the environment.

For this reason, so-called 'smart' wheelchairs are being developed since the early eighties. These systems try to simplify navigation tasks and assist in transporting the user safely to a desired location [5]. Some of the more advanced systems such as TAO,

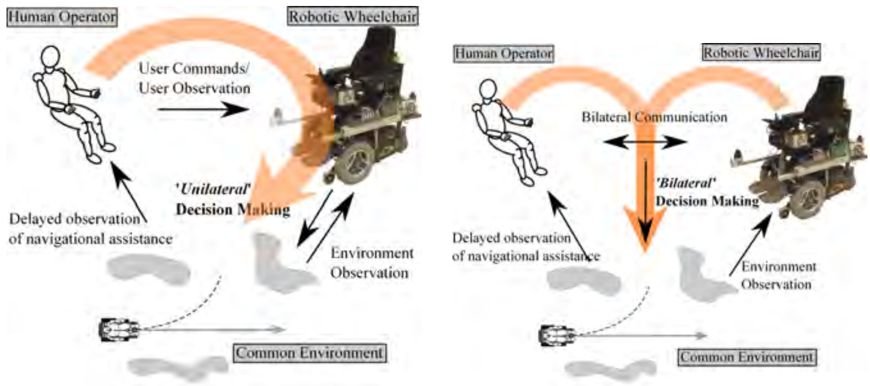

(a) Traditional shared control schemes display asymmetry in the decision making process. Users only understand decisions after actual displacement took place.

(b) Bilateral shared control schemes feature a deeper level of control sharing. The user can negotiate directly with the wheelchair over a haptic communication channel.

Fig. 2. Navigation assistance through unilateral or bilateral shared control

NavChair, Rolland or SmartChair foresee multiple assistance modes that are activated depending on the context. Such systems partially take over the control from the user and adjust the user's inputs by providing assistance for wall-following, collision avoidance or door-passage tasks. Since the user only perceives the decisions by the navigation system *after* wheelchair displacement, such approaches might unexpectedly cause frustration and might actually complicate maneuvering tasks. For instance this is the case when the provided assistance does not correspond to the needed or the expected assistance. The latter is often referred to as *mode confusion* in literature [6, 7]. Shared control approaches that follow this pattern (Fig.2a) exhibit a certain asymmetry in the decision making process and will be referred to as *unilateral* shared control approaches hereafter. With good knowledge of the wheelchair behaviour the user might be able to anticipate the wheelchair's response. Yet, in complex or adaptive assistive schemes this is an error-prone and possibly dangerous process.

To avoid mode confusion problems, researchers started recently to experiment with haptic feedback for wheelchair navigation [8–15] and tele-operated mobile robots [16–18]. By setting up a fast, *bilateral* communication channel between the user and the wheelchair controller, control can be shared more profoundly (Fig.2b). The user can directly negotiate with the controller over this haptic channel and is given the final word, as he/she can *overrule* unwanted wheelchair actions. Next to challenges in designing robust haptic display hardware for this application, a major challenge remains in the design of intuitive bilateral shared control methods that fully exploit the opportunities of the haptic channel and that do not cause additional fatigue of its user. The next section describes a novel haptic navigation assistance strategy that is designed to this end. Experiments, described in section 5 show how this scheme is effectively used to simplify complex maneuvering tasks such as backwards docking into an elevator.

4 Haptic Guidance along Circular Paths

In this section the novel haptic guidance algorithm is introduced. In contrast to earlier works in literature on haptic guidance, the proposed algorithm takes the non-holonomic nature of the wheelchair motion carefully into account. The approach further incorporates the wheelchair's complex (2-dimensional) geometry in order to determine safe passage through confined spaces (subsection 4.1). An adaptive impedance controller is designed (subsection 4.2) to haptically feed the encoded environment information back to the user, assisting him/her to move safely and with confidence.

4.1 Environment Encoding as a Set of Collision-Free Paths

As explained in subsection 2.2, an arbitrary wheelchair trajectory can be seen as a concatenation of multiple circular paths. At each instant of time the user holding the joystick in position (x_j, y_j) commands the wheelchair to move along a path with radius r_m given by (6). The time that the user can hold the joystick in the same position without the wheelchair colliding to an obstacle is a measure of the safety of such a circular path. For example if the distance to an obstacle along this path is large, this path can be considered a relatively *safe* path and the navigation assistance should not interfere. If, on the other hand, the time is short this means that a collision is imminent and haptic guidance away from the collision is required.

Following this principle, the first part of the algorithm encodes the wheelchair's environment as a set of collision-free paths. This takes place as follows:

1. a local map of the environment is built and refined at a fixed update rate. Ranging data from laser sensors together with odometry data is used to build online a map of the environment and to localise the wheelchair within this map. Prior knowledge on the environment can be employed to improve the accuracy of the local map or to speed up the map building process.
2. next, intersections are calculated between the local map and a template of N circular paths departing from the wheelchair. For this, the wheelchair is simulated to follow with a predefined speed (v, ω) each circular path and the earliest time of intersection dt is recorded. These time-values, representative for the collision-free lengths, are stored in an $N \times 1$ vector $\mathbf{dt}$.

Figure 3 depicts an encoding of the environment into a set of collision-free paths.

4.2 Adaptive Impedance Controller to Render Collision-Free Paths

Supplied with a vector of path lengths $\mathbf{dt}$, a model-free impedance controller ([19, 20] displayed in Fig.4), is programmed next. The target impedance $\mathbf{Z}_d$, written in the Laplace domain is:

$$\mathbf{Z}_d(s) = \frac{\mathbf{k}(\phi)}{s} + \mathbf{b}. \tag{7}$$

Both stiffness $\mathbf{k}$ and damping $\mathbf{b}$ contain a radial and a tangential component. The radial component affects the wheelchair speed along a certain trajectory. The tangential

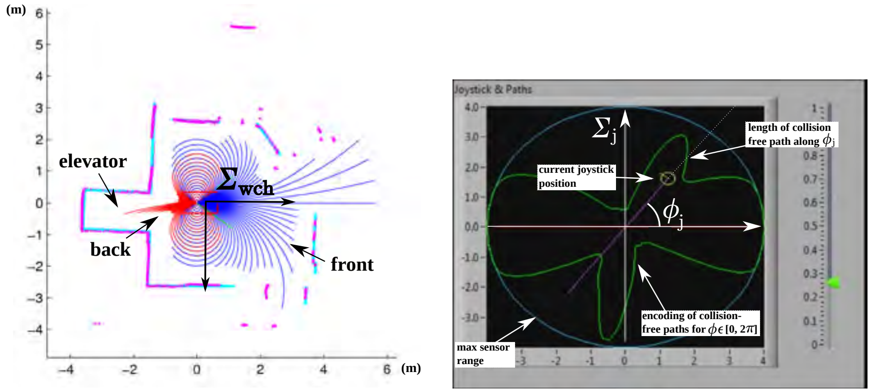

(a) Circular collision-free paths calculated from map (raw sensor data - dark purple dots; prior knowledge - cyan dots), wheelchair geometry (central red rectangle). Blue arcs represent forward paths, red lines are backward paths.

(b) GUI showing encoded environment mapped on joystick frame Σ_j. Small circle represents the joystick position. Lines originating from joystick circle proportional to amplitude of radial and tangential forces.

Fig. 3. Environment encoding as a set of collision-free paths

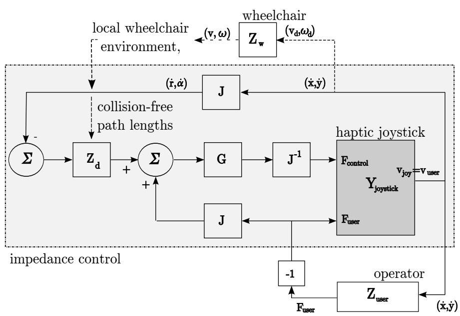

Fig. 4. Impedance controller providing haptic guidance along collision-free paths

component tries to bend the wheelchair motion towards a different circular path. A natural manner to translate collision-free paths towards a stiffness map **k** would exist in attributing higher resistance to shorter collision-free paths and vice versa. In this work a power relation with power p between radial stiffness and path length is employed as described in Table 1. For $p < 1$ the stiffness increases slowly at first and then rises fast when nearing an obstacle. We also performed experiments with a linear relationship between stiffness and collision-free distance. However, in these experiments, we felt that obstacles further away had a relatively large and undesired influence on the stiffness as compared to obstacles nearer by. Given that we do not (yet) take wheelchair velocity into account in the stiffness computation, we found that the polynomial relationship gave better results. Further analysis is deemed necessary to understand this relationship better and see if/how it affects overall system stability.

Table 1. Algorithm 1

Calculating stiffness k_{dt} from path length dt

Input: dt
Output: k_{dt}

if ($dt \geq dt_{max}$)
  $k_{dt} = k_{min}$;
else if ($dt \leq dt_{min}$)
  $k_{dt} = k_{max}$;
else
  $k_{dt} = k_{max} - (k_{max} - k_{min}) \cdot \left(\frac{dt - dt_{min}}{dt_{max} - dt_{min}}\right)^p$;

Under the assumption of perfect masking of joystick dynamics, the radial force displayed to the user is given as:

$$F_r = \begin{cases} -F_{r,0} - k(\phi_j) \cdot r_j - b_r \cdot \dot{r} & \text{for} \quad r \geq r_{nz} \\ -b_r \cdot \dot{r} & \text{for} \quad r < r_{nz} \end{cases} \tag{8}$$

where the joystick position is given as $r_j = \sqrt{x_j^2 + y_j^2}$ and $\phi_j = \tan(y_j, x_j)$. The stiffness $k(\phi_j) = k_{dt}$ for $dt = dt(m)$. The factor b_r is the radial component of the damping $\mathbf{b}$. For stability reasons a neutral zone with radius r_{nz} is programmed around the midpoint in (8). Offset $F_{r,0}$ is such that $F_r|_{(r=r_{nz})}$ is zero, when $\dot{r} = 0$.

In order to pass by an obstacle rather than simply slowing down in front of it, a tangential force F_{ϕ_m} is calculated with central finite differences from the surrounding radial stiffness values as in:

$$F_{\phi_m} = \begin{cases} -F_{\phi_m,0} - \frac{k_{m+1} - k_{m-1}}{\phi_{m+1} - \phi_{m-1}} \cdot r_j - b_\phi \cdot \dot{\phi} & \text{for} \quad r_j \geq r_{nz} \\ -b_\phi \cdot \dot{\phi} & \text{for} \quad r_j < r_{nz} \end{cases} \tag{9}$$

with b_ϕ the tangential component of the damping $\mathbf{b}$ and with joystick angle $\phi_m \in [(m - 1/2)\Delta\phi, (m + 1/2)\Delta\phi)$ for $m = 0, \ldots, N-1$ and $\Delta\phi$ defined in (6). Note that to avoid overly complex notations, the special cases $m = 0, N$ are ignored in (9). The offset $F_{\phi_m,0}$ is a constant such that $F_{\phi_m}|_{(r_j = r_{nz})}$ is zero, when $\dot{\phi} = 0$.

5 Experimental Setup and Validation

5.1 Experimental Setup

To validate the proposed algorithms a test setup was built around a Corpus C500 front-wheel drive wheelchair by Permobil AB. The system is depicted in Fig.5. A metal frame was added to the wheelchair to mount additional hardware. Two Baumer MDFK 10G8124/N64 encoders were integrated on the outgoing axes of the driven wheels. These are used for odometry. Two Hokuyo URG-04LX laser sensors with a field of view of 270° were placed at diagonal corners of this frame. In this way a full 360°

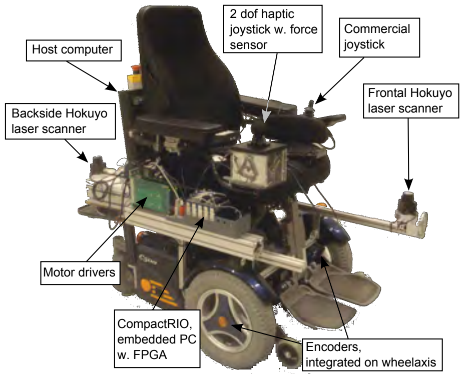

Fig. 5. Permobil Corpus C500 wheelchair interfaced and upgraded for providing haptic navigation assistance

2-dimensional scan of the surroundings of the wheelchair is captured. A host computer mounted at the back of the seating reads out the laser scanners and builds 2D maps of the environment. The host computer communicates over UDP with a NI CompactRIO 9074 central processing unit (cRIO). Labview RT, a real-time OS based upon VxWorks, is installed on this embedded PC. The haptic control loop runs here at a rate of 1kHz. A recent in-house designed 2DOF haptic joystick is mounted in line with the armrest of the wheelchair. This is a compact and powerful joystick showing high continuous output force at the handle (up to 40N, thanks to 2 Maxon RE30 motors, a cable-based reduction mechanism with 1 : 10 reduction ratio and Maxon ADS_E 50/5 PWM current-controlled motor drives). Also, high resolution position measurement (Scancon 2RMHF5000, 20.000 p.p.r. after quadrature encoding) and interaction forces measurements (HBM, 1-LY11-1.5/120 strain gauges glued on the joystick handle) are available.

5.2 Experiment Description

With cardboard boxes an artificial environment was built up to represent an elevator. The user is asked to maneuver the wheelchair backwards inside this elevator starting from a fixed pose. The maneuvering capability with or without navigation assistance is measured during the execution of this task. Parameters that were recorded are time until completion and the number of collisions. At this stage of the research all experiments are conducted by one single able-bodied user (male, 33 years) with limited expertise in conducting powered wheelchairs. Both experiments were conducted 10 times. Three types of experiments were conducted and executed in random order:

type 1: Navigation without Guidance. The user was allowed to look backwards over the shoulder during these experiments. Note that this way of operation is not possible or very tiring for many typical wheelchair users.

type 2: Navigation with Visual Guidance. The user was asked to maneuver the wheelchair while observing the GUI of Fig.3. Guidance forces were calculated and displayed on the GUI (alongside collision-free path lengths) but not applied to the user.

Table 2. Summary of results. (Time in s, average and standard deviation calculated for successful runs only.)

run	1	2	3	4	5	6	7	8	9	10	av.	stdev	coll.
type 1	13.23	13.15	10.11	14.31	11.94	9.45	9.69	10.46	12.07	10.14	11.14	1.47	1
type 2	11.00	12.09	11.47	14.01	9.6	10.34	17.51	11.84	9.82	15.73	11.60	1.48	4
type 3	25.4	10.43	21.86	15.23	19.48	13.37	26.65	13.02	40.83	17.94	18.23	5.89	4

type 3: Navigation under Haptic Feedback. The user was asked to drive 'blindly' inside the elevator solely relying on his sense of touch and the control scheme of section 4. For this, 432 circular paths were used, and the other parameters in Table 1 were: $p = 0.15$, $dt_{min} = 0.3$m and $dt_{max} = 4$m. Some additional precautions were taken. In order to avoid that big jumps in path lengths, due to sensor noise, produce sudden jumps in impedances/and output forces, the circular path data are smoothened by applying a Gaussian convolution mask to vector **dt**. Also, as environment scanning and processing takes place only at a rate of 10Hz, calculated impedance values are upsampled to 1kHz by extrapolating the last two measurements.

5.3 Summary of Results

Table 2 and Fig.6a summarize the results from the different experiments. At this moment, navigating the wheelchair while looking backwards over the shoulder is still superior, but, also here, collisions could not be avoided. Indeed, the task is quite challenging as the elevator is narrow, leaving only about 10cm of space at both sides between wheelchair and door post. With only visual or haptic guidance, the amount of successful executions dropped to $6/10$. This score might seem low, but it must be stressed that the user did not have to look backwards over the shoulder. So such navigation strategy could come in handy to help especially those users that experience problems in looking over their shoulder while steering a wheelchair. Note also that without looking backwards and without guidance successful backwards maneuvering was close to impossible.

At this moment GUI-based navigation is still faster than navigating solely based upon haptic guidance (Table 2). Under haptic guidance the user is somehow 'palpating' the environment to feel where the passage is. The GUI on the other depicts this passage at once, leading to a faster execution. On the other hand, the haptic guidance warns the user when a collision is near. Figure 6b shows an exemplary trajectory where the user turns the wheelchair after such warning and successfully completes the task.

There is still room for improvement. Fig.6c shows that the encoding into circular paths has its limitations. An extension towards other than circular paths will be investigated. Also, at some instants in time, parts of the environment were not observed (Fig.6d). By constructing the wheelchair trajectories from a local map rather than from pure sensory data, paths can be calculated more reliably.

6 Conclusions and Future Work

This article presented a new haptic guidance scheme that is designed to help powered wheelchair users navigate their wheelchair more reliably in their daily environment.

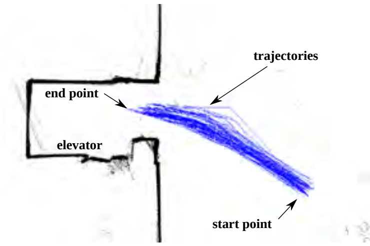

(a) All trajectories of the experiments plotted out. The clock is stopped when the wheelchair's frontal wheels are inside the elevator.

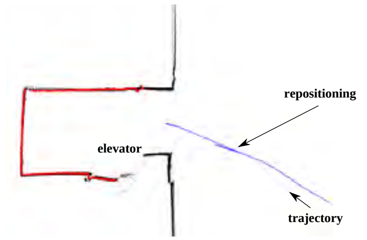

(b) example trajectory under haptic guidance. Through haptic feedback the user turns wheelchair closeby elevator and makes a successful entry

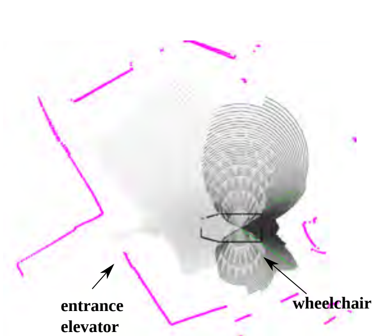

(c) limited guidance when only few circular paths guide towards elevator.

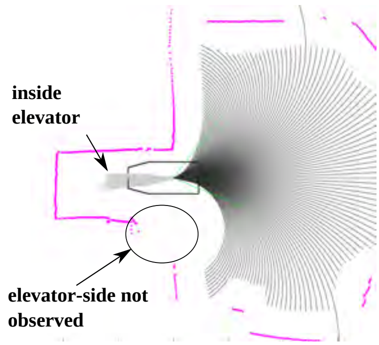

(d) guidance can be wrong when existing obstacles are not observed.

Fig. 6. Navigation trajectories and possible causes of faulty or limited guidance

The guidance scheme contains one component that slows the wheelchair down when approaching an obstacle. Another component bends the wheelchair's motion towards safer paths. The scheme was experimentally validated on a backwards maneuver to drive a wheelchair into an elevator. The results showed that it is feasible to perform such maneuver solely based on haptic guidance, without the user requiring to look backwards over the shoulder or to focus on a GUI screen. Further improvements are still needed however. Improvements could include the use of non-circular paths and the use of the wheelchair's velocity and dynamics in the calculation of the resistance force. Moreover, we would like to test the combination of haptic and visual feedback, and to tune the stiffness-distance relationship further.

Acknowledgments. This research was conducted in the framework of the RADHAR project, funded by the European Commission's 7th Framework Programme FP7/2007-2013 Challenge 2 Cognitive Systems, Interaction, Robotics under grant agreement No. 248873 and under support of a Marie Curie Reintegration Grant, PIRG03-2008-231045. We would also like to thank one anonymous reviewer for the constructive remarks and links to interesting references.

References

1. Powell, D., O'Malley, M.: Efficacy of shared-control guidance paradigms for robot-mediated training. In: World Haptics Conference 2011, Istanbul, pp. 427–432 (June 2011)
2. Matsumoto, Y., Ino, T., Ogusawara, T.: Development of intelligent wheelchair system with face and gazebased interface. In: Proc. of 10th IEEE Int. Workshop on Robot and Human Interactive Communication, pp. 262–267 (2001)
3. Vanacker, G., Millán, J., Lew, E., Ferrez, P., Moles, F., Philips, J., Van Brussel, H., Nuttin, M.: Context-based filtering for assisted brain-actuated wheelchair driving. Computational Intelligence and Neuroscience, Article ID 25 130, 12 pages (2007)
4. Asada, H., Wada, M.: The superchair: A holonomic omnidirectional wheelchair with a variable footprint mechanism. Progress Report, Total Home Automation and Health/Elderly Care Consortium (March 31, 1998)
5. Simpson, R.C.: Smart wheelchairs: A literature review. J. Rehabil. Res. Dev. 42(4), 423–436 (2005)
6. Sheridan, T.: Telerobotics, Automation and Human Supervisory Control. The MIT Press, Cambridge (1992)
7. Lankenau, A.: Avoiding mode confusion in service robots - the bremen autonomous wheelchair as an example. In: Proc. of the 7th Int. Conf. on Rehabilitation Robotics (ICORR 2001), Evry, France, pp. 162–167 (2001)
8. Hong, J.-P., Kwon, O.-S., Lee, E.-H., Kim, B.-S., Hong, S.-H.: Shared-control and force-reflection joystick algorithm for the door passing of mobile robot or powered wheelchair. In: Proc. IEEE Region 10 Conference TENCON 1999, vol. 2, pp. 1577–1580 (1999)
9. Luo, R., Hu, C., Chen, T., Lin, M.: Force reflective feedback control for intelligent wheelchairs. In: Proc. IEEE/RSJ Int. Conf. Intel. Rob. and Syst., pp. 918–923 (1999)
10. Protho, J., LoPresti, E., Brienza, D.: An evaluation of an obstacle avoidance force feedback joystick. In: Conf. of Rehabilitation Engineering and Assistive Technology Soc. of North America (2000)
11. Kitagawa, H., Kobayashi, T., Beppu, T., Terashima, K.: Semi-autonomous obstacle avoidance of omnidirectional wheelchair by joystick impedance control, vol. 4, pp. 2148–2153 (2001)
12. Lee, S., Sukhatme, G., Kim, G., Park, C.-M.: Haptic control of a mobile robot: a user study. Iros 3, 2867–2874 (2002)
13. Fattouh, A., Sahnoun, M., Bourhis, G.: Force feedback joystick control of a powered wheelchair: preliminary study. In: IEEE Int.Conf. on Systems, Man and Cybernetics, vol. 3, pp. 2640–2645 (October 2004)
14. Lee, S., Sukhatme, G.S., Jounghyun, G., mo Park, K.C.: Haptic teleoperation of a mobile robot: A user study. Presence: Teleoperators & Virtual Environments (2005)
15. Bourhis, G., Sahnoun, M.: Assisted control mode for a smart wheelchair. In: IEEE 10th Int. Conf. on Rehabilitation Robotics, ICORR, pp. 158–163 (June 2007)
16. Park, J., Lee, B., Kim, M.: Remote control of a mobile robot using distance-based reflective force. In: IEEE Int'l Conf. on Robotics and Automation, pp. 3415–3420 (September 2003)
17. Diolaiti, N., Melchiorri, C.: Tele-operation of a mobile robot through haptic feedback. In: IEEE Int'l Workshop on Haptic Virtual Environments and Their Applications, pp. 67–72 (2002)

18. Farkhatdinov, I., Ryu, J.-H.: Improving mobile robot bilateral teleoperation by introducing variable force feedback gain. In: IEEE/RSJ Int'l Conf. on Intelligent Robots and Systems, pp. 5812–5817 (October 2010)
19. Tischler, N., Goldenberg, A.: Stiffness control for geared manipulators. In: IEEE International Conference on Robotics and Automation, Proceedings 2001 ICRA, vol. 3, pp. 3042–3046 (2001)
20. Carignan, C., Naylor, M., Roderick, S.: Controlling shoulder impedance in a rehabilitation arm exoskeleton. In: IEEE International Conference on Robotics and Automation, ICRA 2008, pp. 2453–2458 (May 2008)